

Hypervelocity-impact phenomena via molecular dynamics

Brad Lee Holian

Theoretical Division, Los Alamos National Laboratory, Los Alamos, New Mexico 87545

(Received 11 May 1987; revised manuscript received 13 July 1987)

Novel molecular-dynamics calculations have been carried out for a hypervelocity impact of a sphere of 683 atoms (a central atom surrounded by 23 coordination shells) hitting a rectangular plate composed of 8000 atoms (five close-packed planes thick). The ratio of the sphere diameter to the plate thickness was chosen to be approximately 2.4, with the velocity of the sphere chosen such that its kinetic energy was roughly 25 times its binding energy, relative to the bottom of the potential well. Under these conditions, the debris cloud generated by the ball after it penetrates the wall is composed mostly of vaporized material. These microscopic results scale hydrodynamically to macroscopic experiments of a lead sphere hitting a lead plate at 6.6 km/s. There are striking similarities between these atomistic calculations and continuum hydrodynamics simulations, as well as notable differences.

We present here the results of novel molecular-dynamics (MD) simulations of a hypervelocity impact of a sphere of 683 Lennard-Jones particles hitting a plate of 8000 particles. The motivation for such an exercise arises from recent continuum hydrodynamics (hydrocode) simulations of a lead ball striking and penetrating a lead wall at $u_p = 6.6$ km/s.¹ These calculations pointed up a discrepancy between the predicted distribution of mass in the debris cloud and the x-ray photographs² taken at 30 and 40 μ s; namely, the experimental cloud is hollowed out at its center, while the hydrocodes predict a cloud that is densest at the center.

In order to relate the lead-on-lead experiments to time and distance scales appropriate to MD calculations, two parameters are of importance, (1) the ratio of the sphere diameter d to the thickness of the plate, w , and (2) the ratio of the kinetic energy of the impacting sphere, $Nmu_p^2/2$, to its binding, or cohesive energy, NE_{coh} . (The mass of each of the N atoms in the sphere is m .) In the lead-on-lead experiments, the ratio $d/w \simeq 2.4$ (e.g., $d = 1.5$ cm and $w = 0.635$ cm), while $mu_p^2/2E_{\text{coh}} \simeq 25$ (i.e., $u_p = 6.6$ km/s). For the MD calculations, the diameter of the ball ($N = 683$ atoms) was about 10σ (≈ 40 Å), where σ is the crossing point of the pair potential. The wall was composed of five close-packed fcc planes in the x direction (a thickness of about 4.5σ), with a cross-sectional area of $400\sigma^2$. The forward edge of the ball and the back edge of the wall were separated initially by 1.8σ , just beyond the range of the potential. Both the ball and wall were equilibrated at an initial density of $\rho\sigma^3/m = 1$ and temperature, arbitrarily chosen to be about one-tenth the melting point, $k_B T/\epsilon = 0.1$, where ϵ is the well depth of the pair potential. For the truncated Lennard-Jones potential,³ the cohesive energy per atom is about 6ϵ ; hence, the value of $20(\epsilon/m)^{1/2}$ was chosen for u_p . A convenient scale for time is d/u_p , which for the hydrodynamic problem is 2.3 μ s, while for the molecular dynamics problem it is $0.5\sigma(m/\epsilon)^{1/2}$ (consequently, 30 μ s in the hydrodynamics simulation is equivalent to a time of approximately 7 in the MD simulation).

In Fig. 1, we show the initial configuration of the ball and wall for the three-dimensional MD calculations. In Figs. 2–5, the expanding debris cloud is displayed for MD times 1, 2, 4, 5, and 7 (the latter two corresponding roughly to 20 and 30 μ s in hydrodynamics time). In Figs. 1–6, the projection onto the xy plane is shown in (i.e., the side view of the debris cloud as viewed through binoculars from a long distance away); while in Figs. 7–9, the projection onto the yz plane is displayed (i.e., looking at the hole in the wall, as viewed along the path of the ball).

By $t = 2$ (Fig. 3), the debris cloud shows signs of hollowing out in the center. On the surface of the debris bubble are atoms that have been punched out from the plate. The atoms from the sphere are in the forward interior of the cloud. Also, a few atoms from the rear of the ball have been blown off in the opposite direction

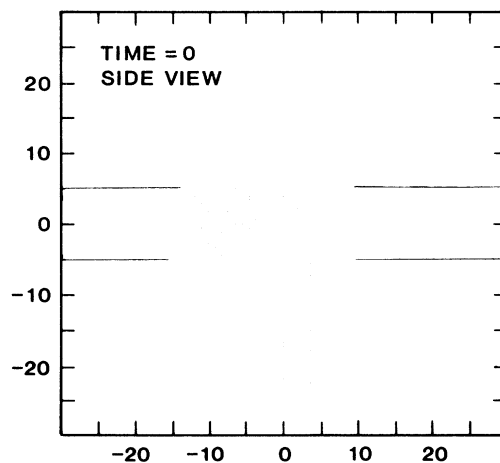


FIG. 1. Side view (xy plane) of the initial configuration (before equilibration) of the 683 ball atoms and 8000 wall atoms. The ball diameter is 10σ and the wall thickness is 4.5σ . (Coordinates on axes in Figs. 1–9 are in units of the crossing point of the pair potential σ .) The initial velocity of the ball is to the right at $20(\epsilon/m)^{1/2}$. Lines indicate the projectile trajectory.

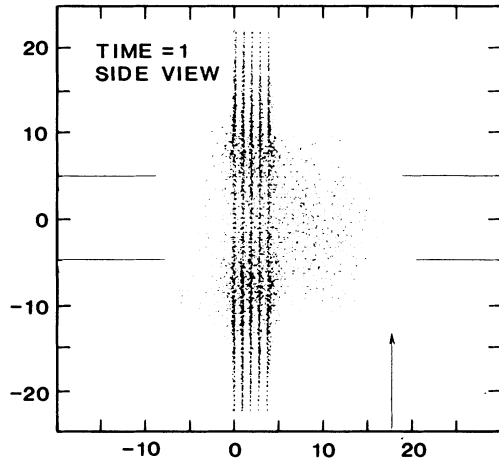


FIG. 2. Side view of the impact at $t = 1$ [the unit of time is $\sigma(m/\epsilon)^{1/2}$]. The arrow shows the leading edge of the ball, had it not hit the wall. A few wall atoms are seen in this region.

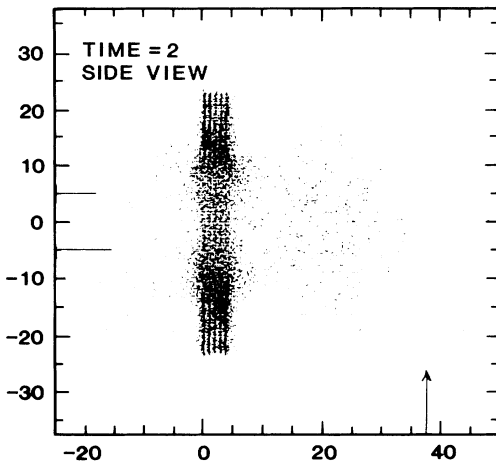


FIG. 3. Side view of the impact at $t = 2$. The lines show the sphere diameter compared to the incipient backplash, hole, and debris bubble. The arrow shows the leading edge of $u_p = 20$ debris atoms.

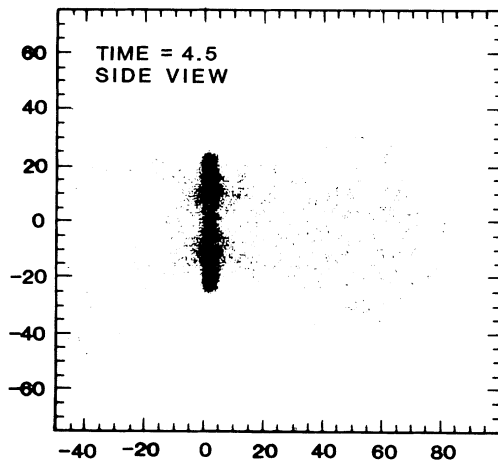


FIG. 4. Side view of the debris cloud at $t = 4.5$.

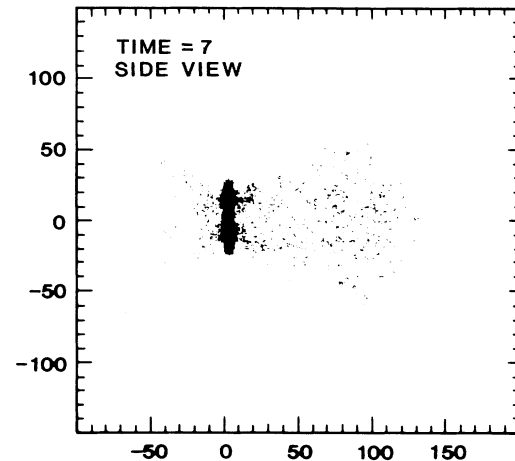


FIG. 5. Side view of the debris cloud at $t = 7$.

from the original projectile velocity, forming the "crown" of the backplash. At $t = 1.5$, the six-fingered shock wave emanating from the hole into the plate (which can be seen at $t = 1$ in Fig. 7), has reached the yz periodic boundaries; the edges of the wall were then set free, and by $t = 2$ rarefaction waves can be seen in Fig. 8 to be moving inward from the edges. Since we are primarily interested in the debris-cloud evolution, we can ignore this perturbation in the wall region. At $t = 4.5$, the distortion on the wall edges is quite pronounced (Fig. 9). An atomistic artifact, which would not be seen in a real polycrystalline lead plate, is the sixfold anisotropy of the diverging shock wave in the MD fcc perfect-crystal plate; an amorphous initial structure would be more realistic in this regard.

By $t = 7$, the debris cloud has developed a mushroom shape, with the beginnings of clusters near the front edges (compare Fig. 5 with Fig. 4). In Fig. 6, the 683

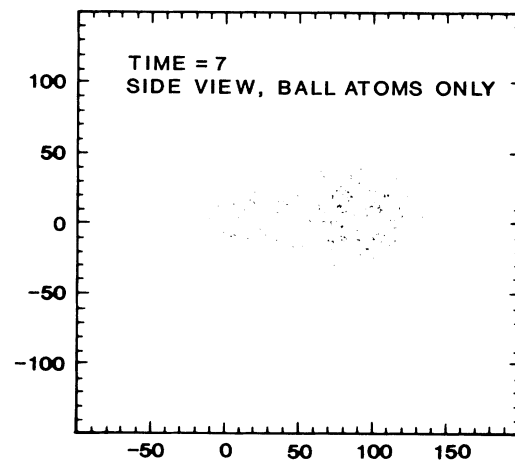


FIG. 6. Side view of the 683 ball atoms at $t = 7$. Compare this with Fig. 5. The cometlike tail comprises the most rearward ($x < 0$) debris, while wall material comprises the most forward, as well as radially most extended, debris atoms. Note the beginnings of condensation of both ball and wall material at the periphery of the cloud. Compare the size of the expanded ball to its size at $t = 0$ (Fig. 1).

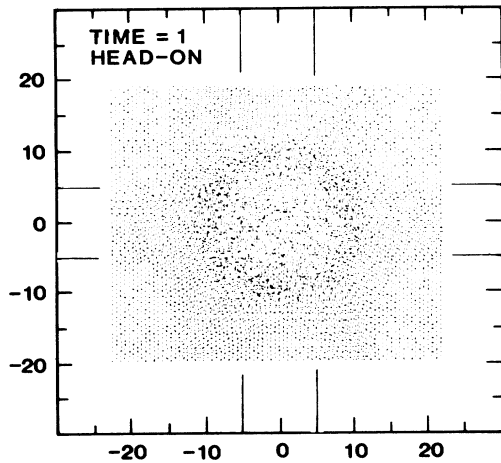


FIG. 7. Head-on view (yz plane) at $t=1$ along the axis of the projectile's path, showing the formation of the hole in the plate. Lines indicate the sphere diameter in comparison with the hole size. Note the shock wave disturbance of hexagonal symmetry in the fcc close-packed planes of the wall.

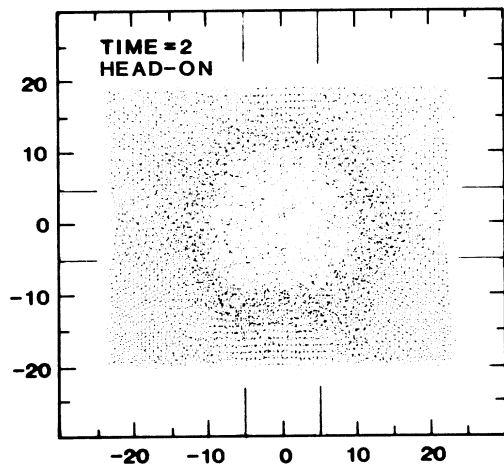


FIG. 8. Head-on view at $t=2$ of the hole. Note the rarefaction waves eating their way inward from the edges of the wall, which by now has free, rather than periodic boundaries.

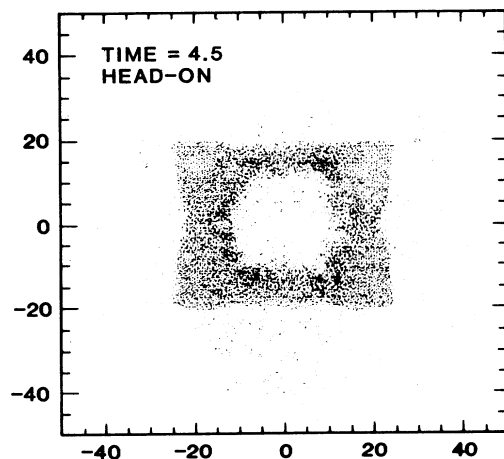


FIG. 9. Head-on view of the hole at $t=4.5$.

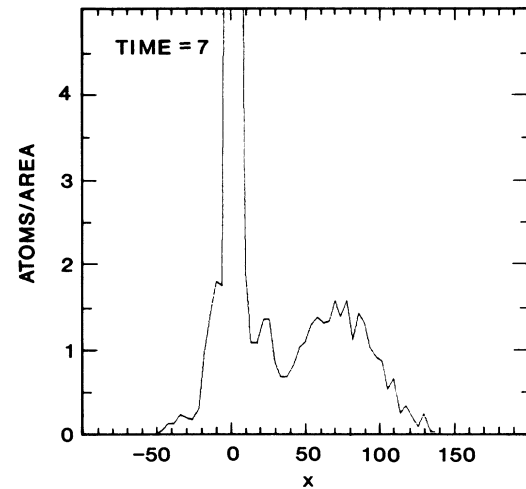


FIG. 10. Mass per unit area (analogous to an x-ray photograph) at $t=7$, projected onto the xy plane along the projectile axis in a strip of width $\Delta y=10\sigma$, with a bin size $\Delta x=4\sigma$.

atoms of the original projectile are shown. We note two interesting features: (1) in comparing Fig. 6 with Fig. 5, we see that the clusters farthest radially from the incident projectile axis are coagulating *wall* particles; and (2) the projectile atoms form a cometlike tail that extends back through the hole and to the farthest reaches rearward. The condensation (clustering) as the debris cloud expands and cools is most interesting and deserving of further investigation.

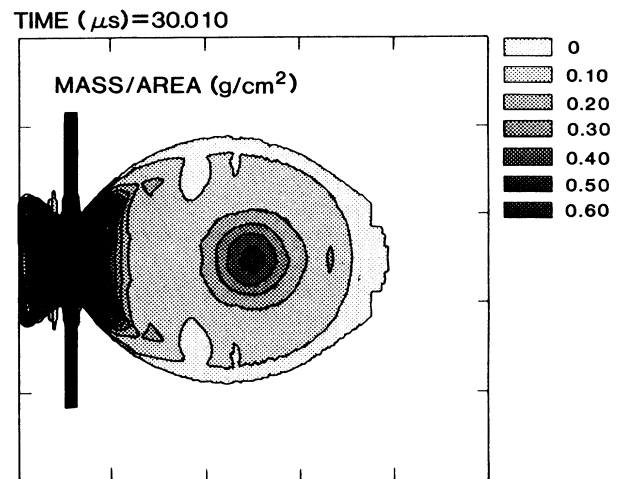


FIG. 11. Two-dimensional, first-order, Eulerian hydrocode calculation (Ref. 1) of the mass per unit area for the lead-on-lead debris cloud (side view) at $30\ \mu\text{s}$. Initially, the 20-g Pb sphere had a diameter of 1.5 cm and was traveling toward the 0.635-cm-thick Pb plate from the left at 6.6 km/s. The front of the debris cloud at $30\ \mu\text{s}$ is approximately 20 cm away from the plate, in fairly good agreement with experiment. To indicate the spatial scale, tic marks have been placed at the borders every 6 cm. Lower limits are indicated for the gray scale, where the darkest part of the simulated x-ray photograph is the most dense region near the plate. Compare with the experimental results in Fig. 12; note that the first-order solution predicts that the cloud is densest at its center.

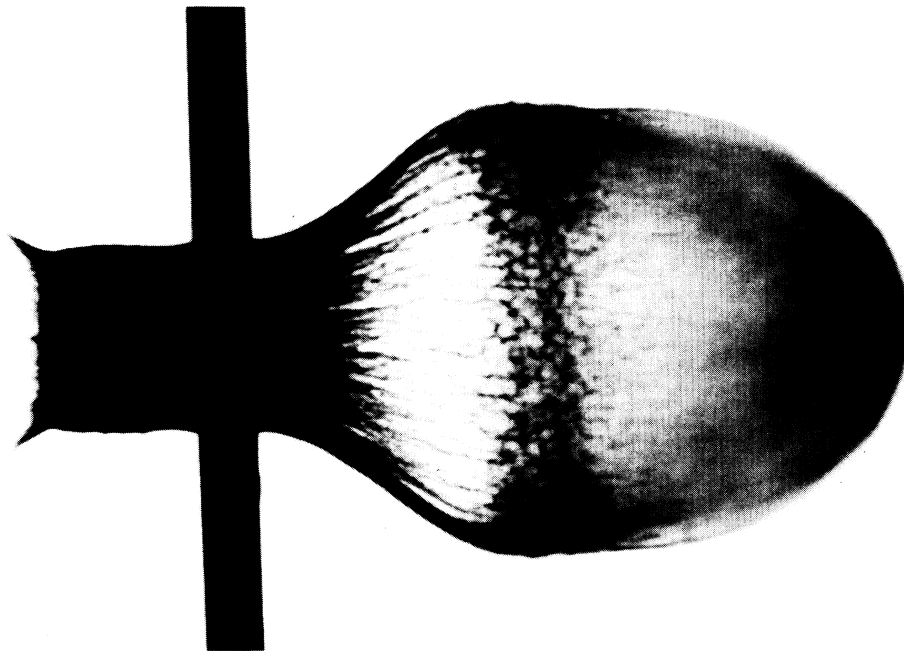


FIG. 12. Experimental x-ray photograph (Ref. 2) of the lead-on-lead debris cloud (side view) at $30 \mu\text{s}$; initial conditions are described under Fig. 11. As in Fig. 11, the darkest regions indicate the highest densities. Note that in contrast to Fig. 11, the experimental cloud is densest at its front and edges. Note also the cylindrical backplash, flared at the edges; rivulets of material, possibly streaming from fractures at the edges of the hole in the plate, ending in a collar at the rear of the cloud; and the cylindrical midsection of the debris cloud. The outline of the MD cloud (Fig. 5) more closely resembles experiment than the hydrocode calculation (Fig. 11), except for the backplash.

In general, the MD results mirror those of the hydrocodes, even though the physical scale of these atoms is many orders of magnitude smaller. That hydrodynamic (continuum) behavior extends downward to such small time and distance scales is, by now, a well-known feature of atomistic simulations.⁴ Displayed in Fig. 10 is the mass per unit area of the debris cloud for a strip of width $\Delta y = 10\sigma$, projected onto the xy plane. The large peak near $x = 0$ is the plate; hollowing out of the debris cloud is occurring just forward of the plate. The peak at the center of the cloud is primarily composed of ball atoms. Like the hydrocode calculations,¹ an example of which is shown in Fig. 11, the MD cloud is densest at the middle, and in this important respect does not resemble the experimental results² shown in Fig. 12. The reason that the hydrocode fails to reproduce the experiment is that there are advection errors in the first-order Eulerian solution, which are known to smear out features such as a shell of material; an order of magnitude smaller mesh size, or higher-order treatment of the advection may solve this difficulty.¹ For atomistic as op-

posed to continuum simulations, however, it is important to remember that there is an extra distance scale, namely, the range of the pairwise interaction potential σ . Until an order of magnitude more ball atoms is simulated, we can expect MD calculations to appear inherently more "gluey" than an accurate continuum treatment; that is, compared to blobs of continuum, the atoms in these MD calculations tend to cluster more easily in the final stages of the debris-cloud expansion, as well as failing to fragment as easily in the early stages of the bubble formation.

It is a pleasure to thank Kathy Holian (Los Alamos), Norm Johnson (Los Alamos), Tim Trucano (Sandia Labs, Albuquerque), and Joe Beeler (North Carolina State University) for sharing their ideas on this very interesting problem, as well as Bill Hoover (Livermore) for his helpful comments and suggestions. Work performed under the auspices of the University of California for the U. S. Department of Energy, Contract No. W-7405-Eng-36.

¹K. S. Holian and M. W. Burkett, *Int. J. Impact Eng.* **5**, 333 (1987).

²G. W. Pomykal, Lawrence Livermore Laboratory Report No. DDV-86-0010, 1986 (unpublished). The x-ray photograph shown in Fig. 12 was taken at GM Delco (Santa Barbara, California) by D. J. Liquornik.

³B. L. Holian and D. J. Evans, *J. Chem. Phys.* **78**, 5147 (1983). The truncated Lennard-Jones pair potential is modified at

separations larger than the distance of maximum attractive force by matching a cubic spline at that point (1.24σ) out to the maximum (1.74σ), where both the potential and force go smoothly to zero.

⁴For an interesting review of the relationship of the atomistic to the continuum world, see W. G. Hoover, *Phys. Today* **37**(1), 44 (1984).

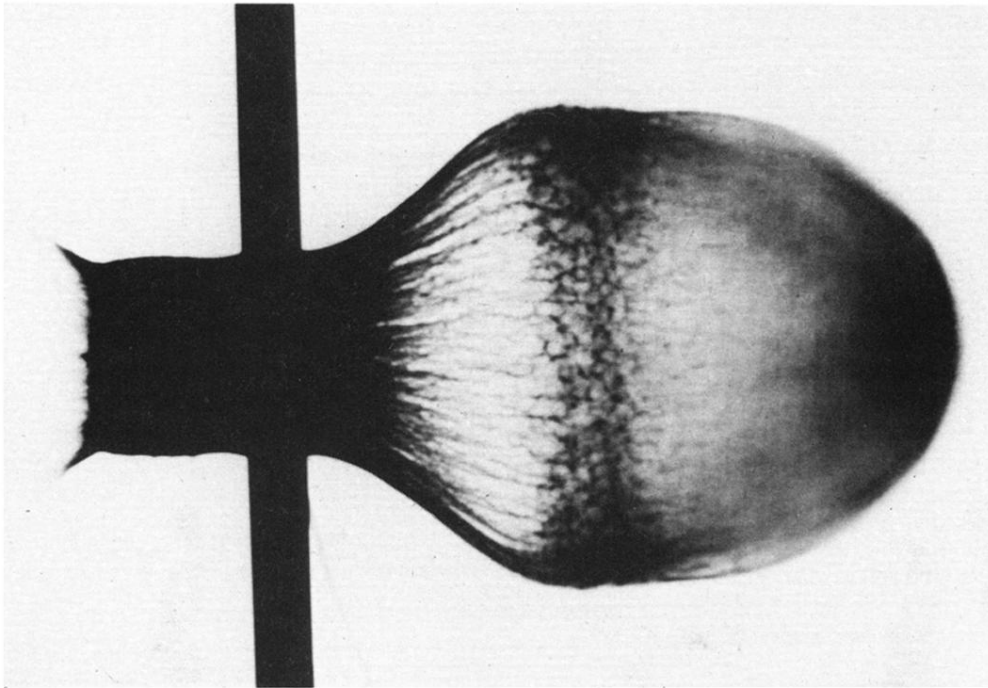


FIG. 12. Experimental x-ray photograph (Ref. 2) of the lead-on-lead debris cloud (side view) at $30 \mu\text{s}$; initial conditions are described under Fig. 11. As in Fig. 11, the darkest regions indicate the highest densities. Note that in contrast to Fig. 11, the experimental cloud is densest at its front and edges. Note also the cylindrical backslash, flared at the edges; rivulets of material, possibly streaming from fractures at the edges of the hole in the plate, ending in a collar at the rear of the cloud; and the cylindrical midsection of the debris cloud. The outline of the MD cloud (Fig. 5) more closely resembles experiment than the hydrocode calculation (Fig. 11), except for the backslash.